Identification of a novel basal body-localized epsilon-tubulin in *Leishmania*

Arunava Seth[*1], Anubhab Das[#1] and Rupak Datta[*1]

[1]Department of Biological Sciences, Indian Institute of Science Education and Research (IISER) Kolkata, Mohanpur, West Bengal, India.

*Corresponding authors:

Rupak Datta

Email: rupakdatta@iiserkol.ac.in

ORCID ID- 0000-0003-1820-9251

Arunava Seth

Email: as16ip009@iiserkol.ac.in

ORCID ID- 0000-0001-8544-3457

#Worked at the Department of Biological Sciences, IISER Kolkata as a summer intern; present address: Department of Ophthalmology, Visual and Anatomical Sciences, Wayne State University School of Medicine, Detroit, MI, USA

Running title: Epsilon tubulin of *Leishmania*

Keywords: Epsilon-tubulin, *Leishmania*, tubulin, cytoskeleton, basal body, nocodazole

Summary Statement

We report for the first time an epsilon-tubulin in *Leishmania* parasite. This nocodazole-insensitive unconventional tubulin is expressed constitutively and found to be localized in the basal body.

Abstract

Epsilon-tubulin is an unconventional isoform of the tubulin family, found in only a few organisms so far. We identified a novel epsilon-tubulin in *Leishmania major* (Lmε-tubulin) that exhibits significant sequence similarity and conservation of functional domains with its known counterparts. Lmε-tubulin was found to be constitutively expressed in both the extracellular promastigote form of the parasite and the amastigotes residing within infected macrophages. For localization studies, we generated a *Leishmania* strain expressing mNeonGreen-tagged Lmε-tubulin using CRISPR-Cas9-mediated endogenous protein tagging method. Imaging studies with this strain revealed Lmε-tubulin to be localized near the kinetoplast and at the flagellar base, indicating a basal body localization. That Lmε-tubulin is indeed localized at the basal body and not a part of the microtubular network was confirmed when its localization was found to remain unaltered upon treatment with nocodazole, a microtubule disruptor. This is the first report of ε-tubulin not only in the genus *Leishmania* but in the entire *Trypanosomatidae* family and is likely to incite further research to uncover the physiological role of this intriguing tubulin in this group of protozoan parasites.

Introduction

Leishmania species are causal agents for leishmaniasis, a group of diseases with diverse clinical manifestations. Depending on the species involved, the symptoms of leishmaniasis can range from fatal infections of the spleen and liver to self-resolving skin lesion (Burza et al., 2018). Despite this diversity of symptoms, all *Leishmania* species share a similar digenetic life cycle involving a sandfly vector, typically from the genus *Phlebotomus* or *Lutzomyia*, and a mammalian host such as humans. During this lifecycle, the parasite switches between two distinct morphological forms. In the insect stage, it appears as a long, slender promastigote with a motile flagellum. After infecting the host macrophages, the promastigotes transform into small, rounded amastigotes with short, non-motile flagellum. This promastigote-to-amastigote transition is crucial for the survival of intracellular *Leishmania*. The drastic morphological changes involved in this process requires substantial cytoskeletal restructuring (Gluenz et al., 2010; Sunter and Gull, 2017).

Tubulins, along with actin, are pivotal in regulating cytoskeleton dynamics. They play crucial roles in various cellular functions such as vesicular trafficking, cell shape maintenance and cell cycle progression in most eukaryotic cells, including lower eukaryotes like *Leishmania* (Dandugudumula et al., 2022; Fourriere et al., 2020; Gull, 1999; Janke and Chloë Bulinski, 2011; Pollard and Cooper, 2009). Microtubule organizing centers (MTOCs) are the primary nucleation sites for tubulin polymerization. The MTOCs exist in different forms, such as basal bodies associated with cilia or flagella, and centrosomes linked to mitotic spindles (Wu and Akhmanova, 2017). In *Leishmania* as well as in other members of the *Trypanosomatidae* family, the basal body is closely associated with the kinetoplast near the flagellar pocket, a site through which processes like endocytosis or exocytosis occur (Field and Carrington, 2009; Overath et al., 1997; Sengupta et al., 1999; Stierhof et al., 1994). It also plays critical role in

formation and anchoring of the flagellum thereby acting as controlling center for parasite's motility, attachment and infectivity (Halliday et al., 2020; Sunter et al., 2019).

The *Leishmania* basal body is reported to have the classical 9+2 arrangement of microtubules in the promastigote form and a 9+0 arrangement in the amastigotes (Alexander, 1978; Rudzinska et al., 1964; Wheeler et al., 2015). Limited investigations on the *Leishmania* basal body composition have so far identified only a few key proteins, such as centrin, centrin4, protein of centriole, and SAS6 (Selvapandiyan et al., 2001; van Breugel et al., 2014; Vats et al., 2023). Apart from these, γ-tubulin is also known to localize in its basal body (Libusová et al., 2004). In contrast, alpha and beta-tubulin of *Leishmania* act as monomers for protofilaments forming microtubules but are not part of the basal body (Fong and Lee, 1988; Wirth and Slater, 1983). However, the presence of other unconventional tubulin isoforms, such as epsilon, delta, and zeta tubulins, remains to be experimentally validated in *Leishmania* as well as in other parasites of the *Trypanosomatidae* family.

The epsilon, delta, and zeta-tubulins, collectively grouped as evolutionary co-conserved ZED module, are predicted to be present in most eukaryotes, ranging from unicellular protists to higher-order mammals (Turk et al., 2015). Interestingly, genome analysis across various organisms revealed a unique pattern of conservation of the ZED module tubulins. It was observed that organisms lacking epsilon-tubulin were also missing delta and zeta-tubulins, while those possessing epsilon-tubulin consistently had delta and/or zeta-tubulin as well. This observation suggests that epsilon-tubulin might be playing a central role in coordinating the function of ZED module, acting in partnership with delta and/or zeta-tubulin (Turk et al., 2015).

Epsilon-tubulin was first predicted in *Saccharomyces cerevisiae* by RG Burns through extensive bioinformatic analysis (Burns, 1995). Subsequently, it was discovered in many other organisms, including humans (Chang and Stearns, 2000; Dupuis-Williams et al., 2002; Dutcher et al., 2002; Ross et al., 2013). In human cells, the epsilon-tubulin was found to localize in the

centrosome but at a distinct site from γ-tubulin (Chang and Stearns, 2000). Epsilon-tubulin from *Xenopus laevis*, which is similar to its human counterpart in terms of sequence and localization, has been reported to be important for centriole duplication (Chang et al., 2003). The basal body-localized epsilon-tubulin of *Paramecium* was found to play essential role in the assembly and anchorage of the centriolar microtubules (Dupuis-Williams et al., 2002). In *Tetrahymena thermophila*, deletion or mutation of the epsilon-tubulin gene caused flagellar defects, with some mutations proving to be lethal (Ross et al., 2013). Similarly, in *Chlamydomonas*, deletion of epsilon-tubulin resulted in failure in basal body assembly, preventing proper flagella formation (Dutcher et al., 2002). Despite these studies proving the essentiality of epsilon-tubulin in various organisms across different branches of life, its presence in the *Trypanosomatida* group of protozoan parasites remains ambiguous. Although Vaughan *et. al.* have bioinformatically predicted the presence of epsilon-tubulin in *Trypanosoma brucei*, its experimental validation is still awaited (Vaughan et al., 2000). Till date, there is no report on epsilon tubulin in any of the *Leishmania* species.

We report here identification of an epsilon-tubulin in *Leishmania major* (*L. major*), which exhibited constitutive expression in both the extracellular promastigote and intracellular amastigote forms of the parasite. Using CRISPR-Cas9 mediated endogenous protein tagging, coupled with imaging studies, we demonstrated that this nocodazole-insensitive unconventional tubulin is localized at the basal body. This is the first experimentally validated epsilon tubulin in the entire *Trypanosomatida* family. This discovery is likely to encourage further structure-function studies aimed at understanding the role of epsilon tubulin in parasite physiology.

Results and Discussion

Identification of *L. major* epsilon-tubulin

115 Genome sequence of *L. major* predicted the presence of a putative epsilon-tubulin on
116 chromosome 21, annotated as LmjF.21.1010 (Ivens, 2005). The predicted protein sequence of
117 *L. major* epsilon-tubulin (Lmε-tubulin) was aligned with bona fide, well-characterized epsilon-
118 tubulins from *Tetrahymena thermophila* (Ross et al., 2013), *Chlamydomonas reinhardtii*
119 (Dutcher et al., 2002), *Homo sapiens* (Chang and Stearns, 2000) and *Paramecium tetraurelia*
120 (Dupuis-Williams et al., 2002) (Fig 1). Lmε-tubulin was found to share ~ 40% sequence
121 identities and ~ 60% sequence similarities with its counterparts in these species (Fig 1, Table
122 S1). InterPro analysis confirmed the presence of signature tubulin domains, the GTPase domain
123 and C-terminal domain, in Lmε-tubulin (Fig 1; yellow and green shaded regions) (Nogales et
124 al., 1998a; Nogales et al., 1998b; Paysan-Lafosse et al., 2023). Importantly, 23 out of 27 GTP-
125 binding residues of *Tetrahymena* epsilon-tubulin are either conserved or replaced with similar
126 residues in Lmε-tubulin (Fig 1; black triangles). Also, nine out of ten amino acids, mutations
127 of which in *Tetrahymena* epsilon-tubulin led to lethal or slow-growing phenotypes, were found
128 to be conserved in Lmε-tubulin (Fig 1; black boxes) (Ross et al., 2013). Studies with
129 *Paramecium* and Human epsilon-tubulins revealed that they have unique amino acid insertions,
130 which are absent in canonical tubulins (Dupuis-Williams et al., 2002; Inclán and Nogales,
131 2001). These insertions were hypothesized to be required for longitudinal contact with other
132 tubulins (Inclán and Nogales, 2001). We probed for the presence of such insertions in Lmε-
133 tubulin by aligning its sequence with α, β and γ-tubulins of *L. major* (Fig S1A). Most of the
134 regions aligned except two prominent stretches of amino acids; Insertion I (R211 - T236) and
135 Insertion II (H325 - T332) (Fig S1A). Comparison of the AlphaFold structure of Lmε-tubulin
136 with that of the structures of α, β and γ-tubulins of *L. major* showed mostly aligned regions,
137 except for the insertions I and II (Fig S1B). The sequence and structural alignment results thus
138 confirmed the presence of these characteristic insertions in Lmε-tubulin. Interestingly, we
139 observed that the C-terminal of the Lmε-tubulin also did not align properly with the α, β or γ-

140 tubulins (Fig S1B). The C-terminal residues of canonical tubulins are reported to be crucial for
141 post-translational modifications (Janke and Chloë Bulinski, 2011). So, a lack of proper
142 alignment and absence of secondary structure of Lmε-tubulin C-terminal region suggests that
143 the post-translational modifications are either absent or different from the classical tubulins. A
144 similar feature was earlier observed in the C-terminal domain of *Tetrahymena* epsilon-tubulin
145 (Ross et al., 2013). Isoforms of Lmε-tubulin were also predicted in the genomes of other
146 *Leishmania* species, each displaying very high sequence identity (>97% for *L. donovani*, *L.*
147 *infantum*, *L. mexicana* and >90% for *L. braziliensis)* (Table S1). Lmε-tubulin was found to
148 exhibit >65% sequence identity and >80% sequence similarity with putative epsilon tubulins
149 of other members of the *Trypanosomatida* family, *T. brucei* and *T. cruzi* (Table S1).
150 Collectively, these findings from our bioinformatic analyses strongly affirm the legitimacy of
151 Lmε-tubulin as an authentic epsilon tubulin.

152 **Promastigote and amastigote forms of *L. major* both expresses epsilon-tubulin**

153 Analysis of the genetic locus revealed that the *Lmε-tubulin* is flanked upstream by a
154 hypothetical gene (LmjF.21.1000) and downstream by the putative dynein arm light chain
155 encoding gene (LmjF.21.1020) (Fig 2A). To experimentally verify the presence of *Lmε-tubulin*
156 in the genome, we used *L. major* genomic DNA as the template for PCR amplification of the
157 corresponding segment using *Lmε-tubulin*-specific primers (P1 & P2). A 1413 bp product was
158 obtained, which matched with the expected size of *Lmε-tubulin* coding region (Fig 2B). After
159 confirming the presence of *Lmε-tubulin* in the genome, our next goal was to check its
160 expression. For this, cDNAs, prepared from *L. major* promastigote mRNAs, were subjected to
161 PCR amplification with primers, P1 & P2. This RT-PCR yielded 1413 bp product, confirming
162 the expression of Lmε-tubulin mRNA in the promastigote stage (Fig 2C). Since many genes of
163 *Leishmania* exhibit stage-specific expression pattern, we wanted to verify whether Lmε-tubulin
164 is expressed in the intracellular amastigote form also (Brotherton et al., 2010). For this, as

165 described schematically in Fig 2E, we infected J774A.1 macrophage cells with *L. major*
166 promastigotes and isolated total mRNAs from the infected macrophages at ~ 60 hours post-
167 infection (to allow promastigote-to-amastigote transformation). This pool of mRNA was a
168 mixture derived from both host macrophage cells and the intracellular amastigotes. When RT-
169 PCR was performed with primers P1 & P2 using this mRNA pool from the *Leishmania* infected
170 macrophages, a 1413 bp product got amplified confirming the presence of Lmε-tubulin
171 transcripts in the amastigotes. That this product was not a non-specific amplification from
172 macrophage mRNA was confirmed when we found that mRNA isolated from uninfected
173 macrophages did not yield any product upon RT-PCR (Fig 2E).

174 **CRISPR-Cas9 mediated tagging of endogenous epsilon-tubulin with mNeonGreen**

175 Determining the localization of a protein is a prerequisite to understand its function. To
176 examine the localization of Lmε-tubulin, we planned to tag the endogenous protein with the
177 fluorophore mNeonGreen using CRISPR-Cas9 gene editing technology (Beneke et al., 2017).
178 For this, we first generated an *L. major* strain expressing *Streptococcus pyogenes* Cas9
179 (SpCas9) and T7 Polymerase (T7Pol). The strain was verified using genomic DNA PCR, using
180 primers specific for SpCas9 and T7pol. This produced 4.1 kb and 2.7 kb PCR products,
181 respectively, confirming successful integration of SpCas9 and T7pol in the *L. major* genome
182 (Fig S2). This strain, referred to as LmCas9:T7Pol, was used to generate the N-terminal
183 mNeonGreen (mNG)-tagged-Lmε-tubulin expressing *L. major* (Fig 3A), as described in details
184 in the materials and methods section and in Fig S3. When the whole cell lysate of this
185 engineered strain was subjected to western blot with anti-mNG antibody, an 81.7 kDa band
186 corresponding to the molecular weight of the fusion protein (30 kDa: 3XMyc-mNeonGreen,
187 and 51.7 kDa: Lmε-tubulin) was observed. As expected, no band was observed when similar
188 western blot was performed with the lysates from control cells (wild type *L. major* or
189 LmCas9:T7Pol) (Fig 3B).

190 **The epsilon-tubulin is localized at two distinct spots in the basal body of *L. major***

191 After successful validation of the (mNG)-tagged-Lmε-tubulin expression *L. major* strain, we
192 aimed to determine intracellular localization of Lmε-tubulin in both promastigotes and
193 intracellular amastigotes. Confocal microscopy of the (mNG)-tagged-Lmε-tubulin expressing
194 *L. major* promastigotes revealed two bright fluorescent spots in the cell body, one in close
195 association with the kinetoplast DNA and the other at the base of the flagella (Fig 3C). Such a
196 distinct pattern of fluorescent signal indicates basal body localization of Lmε-tubulin. The
197 localization pattern of Lmε-tubulin is reminiscent of centrin, another basal body-localized
198 protein of the parasite (Selvapandiyan et al., 2001). To check the localization of Lmε-tubulin
199 in the intracellular amastigote stage, confocal images were acquired directly from the J774A.1
200 macrophages infected with the (mNG)-tagged-Lmε-tubulin expressing *L. major* strain. Such
201 direct image acquisition method ensures authenticity of the amastigote-character of the
202 parasite, which could otherwise be altered if amastigotes were isolated from the infected
203 macrophages prior to imaging. Like in promastigotes, two distinct fluorescent spots in close
204 proximity of the kinetoplast and the flagellar base were observed in the amastigotes as well
205 (Fig 3D).

206 To validate basal body localization Lmε-tubulin, we treated the (mNG)-tagged-Lmε-tubulin
207 expressing *L. major* promastigotes with nocodazole, a known microtubule depolymerizer that
208 does not disrupt the basal body structure. Previous studies in U2OS cells have demonstrated
209 that nocodazole treatment does not affect the localization of human epsilon and delta tubulins,
210 as they are associated with the centrosome and are not part of the microtubular network (Chang
211 and Stearns, 2000; Debrabander et al., 1977). We observed that the localization of Lmε-tubulin
212 indeed remained unchanged in >90% of the cells upon treatment with 1 μM nocodazole (Fig
213 4A, B). To rule out the possibility that nocodazole does not work on *Leishmania* cells, we
214 decided to perform a control experiment to verify if nocodazole treatment could disrupt the

localization of α-tubulin, which is an integral part of the microtubular network (McKenna et al., 2023). For this, we generated a mNG- α-tubulin *L. major* strain following similar CRISPR-Cas9-based gene editing method. The authenticity of the strain was confirmed by western blot with anti-mNG antibody, showing a 79.7 kDa band corresponding to the fusion protein (Fig S4). The untreated mNG-α-tubulin in *L. major* promastigotes exhibited characteristic microtubule localization pattern, predominantly along the periphery of the cell, as previously reported earlier in *L. mexicana* (Tran et al., 2015). When these cells were treated with nocodazole, it was observed that unlike the Lmε-tubulin, which was largely insensitive to the drug, the α-tubulin localization pattern drastically changed due to microtubule disassembly (Fig 4C, D). Taken together, these data provided unambiguous evidence that Lmε-tubulin is indeed localized at the basal body and not part of the broader microtubular network. In this context it is worth mentioning that epsilon tubulin isoforms from *Tetrahymena*, *Chlamydomonas*, *Paramecium* and human have been also shown to localize in the basal body (Chang and Stearns, 2000; Dupuis-Williams et al., 2002; Dutcher et al., 2002; Ross et al., 2013). This suggests that Lmε-tubulin may share functional similarity with its counterparts in these organisms.

In conclusion, we identified for the first time a constitutively expressed, basal body-localized ε-tubulin not only in the genus *Leishmania* but in the entire *Trypanosomatidae* family. However, further studies, including genetic knockout of Lmε-tubulin, are necessary to definitively establish the role of this unconventional tubulin in basal body stability and maintenance. It will be also important to investigate Lmε-tubulin's interaction of with other tubulin isoforms to gain a comprehensive understanding of the microtubule dynamics, particularly during promastigote-to-amastigote transition. The CRISPR-Cas9 mediated tagging method employed here to label endogenous Lmε-tubulin can prove to be very useful for

239 detailed study of the basal body architecture and in identifying different proteins associated
240 with it. Thus, our work is likely to stimulate further research towards these directions.

241 **Material and Methods**

242 All reagents were purchased from Sigma-Aldrich unless otherwise mentioned. Primers used
243 for PCR were obtained from Integrated DNA Technologies and their sequence information are
244 provided in Table S2. Details of antibodies used in this study are mentioned in Table S3.

245 ***Leishmania* and mammalian cell culture**

246 *L. major* strain (MHOM/SU/73/5-ASKH) and J774A.1 murine macrophages were procured
247 from ATCC. *L. major* promastigotes were cultured as described before (Pal et al., 2015).
248 Briefly, *L. major* cells were grown at 26 ^{0}C in M199 medium (Gibco) supplemented with 15%
249 heat-inactivated fetal bovine serum (Gibco), 23.5 mM HEPES, 0.2 mM adenine, 150 µg/ml
250 folic acid, 10 µg/ml hemin, 120 U/ml penicillin, 120 µg/ml streptomycin, and 60 µg/ml
251 gentamicin. J774A.1 murine macrophages were cultured in Dulbecco's modified Eagle's
252 medium (Gibco) pH 7.4, supplemented with 10% heat-inactivated fetal bovine serum, 2 mM
253 L-glutamine, 100 µg/ml streptomycin and 100 U/ml penicillin at 37 °C in a humidified
254 atmosphere containing 5% CO_2. Whenever necessary, a hemocytometer was used to count cells
255 fixed with 0.9% formal saline or stained with Trypan blue.

256 **Sequence alignment and bioinformatics**

257 Sequence alignment was performed using the Clustal Omega
258 (https://www.ebi.ac.uk/jdispatcher/msa/clustalo). NCBI Blast (https://blast.ncbi.nlm.nih.gov/
259 Blast.cgi) was used to determine the percent identity and similarity. The result was copied and
260 modified for presentation using MS Word processor and Inkscape without changing any base
261 value. Mutated residues were manually colored as per the literature (Ross et al., 2013) and the
262 tubulin mutation database (https://tubulinmutations.bio.uci.edu/.html). Domains were
263 predicted based on InterPro analysis (https://www.ebi.ac.uk/interpro/). The following protein

264 sequences were obtained from UniProt, epsilon-tubulins from *L. major* (Q4QC95), *T.*
265 *thermophila* (Q22YZ9), *C. reinhardtii* (A0A2K3DX56), *Homo sapiens* (Q9UJT0),
266 *Paramecium tetraurelia* (Q8WPW7), *L. donovani (A0A3Q8IAD6), L. mexicana* (E9AV85)*, L.*
267 *braziliensis* (A4HBW1)*, L. infantum* (E9AGW9)*, T. cruzi* (A0A7J6XYD9)*, T. brucei*
268 (Q9NI44) *L. major* α-tubulin (Q4QGC5), *L. major* β-tubulin (Q4Q4C4), *L. major* γ-tubulin
269 (Q4Q9Z8). The predicted structure for *L. major* α-, β- and γ-tubulin was obtained from the
270 AlphaFold server (Jumper et al., 2021; Varadi et al., 2022). Structural alignment was done using
271 the ChimeraX software module (Pettersen et al., 2004).

272 **Genomic DNA PCR**

273 The genomic DNA of *L. major* promastigotes was isolated using the phenol-chloroform
274 method. Briefly, 1 x10^7 *L. major* cells were harvested and resuspended in 0.1 ml lysis buffer
275 (0.1 M Tris-Cl, 0.1 M NaCl, 1% SDS, 100 mM EDTA, 100 µg/ml Proteinase K) and incubated
276 at 55 ^{0}C for 120 minutes. 25 µl phenol and 25 µl chloroform were added to the lysate and
277 centrifuged at 13000g for 15 minutes. The upper aqueous phase was taken in a fresh tube, and
278 an equal volume of chloroform was added and centrifuged at 13000g for 15 minutes. The
279 supernatant was collected, and 1/10 volume 3 M sodium acetate and 2 volume ethanol were
280 added and centrifuged at 13000g for 10 minutes. The pellet is washed with 70% ethanol twice
281 and eluted in nuclease-free water. DNA Concentration was determined spectrophotometrically
282 using NanoDrop spectrophotometer. Genomic DNA PCR amplification was performed using
283 Leo Mastermix (Dxbidt, India) and specific primers following manufacturer's protocol.

284 **Checking of Lmε-tubulin expression in *L. major* promastigote**

285 Total RNA from *L. major* promastigotes was isolated using Trizol reagent (Invitrogen)
286 followed by DNase I treatment (Invitrogen). cDNA was prepared from DNase I-treated RNA
287 using Verso cDNA kit (Thermo Scientific) using the manufacturer's protocol. -RT controls
288 were prepared from DNase I treated RNA where all Verso cDNA kit components were added

289 except the reverse transcriptase enzyme. PCR was performed using the cDNAs from +RT and
290 -RT samples.

291 **Checking of Lmε-tubulin expression in *L. major* amastigote**

292 *L. major* infection of J774A.1 macrophages was performed as described by us before (Pal et
293 al., 2017). Briefly, J77A.1 macrophages were activated in the presence of 100 ng/ml LPS for 6
294 hours, and to it stationary phase *L. major* cells were added at MOI 1:30. After 12 hours, media
295 was discarded to remove uninternalized parasites, and washed with 1X PBS, and fresh DMEM
296 media was added, and incubated for ~60 hours. Total RNA was extracted from infected and
297 uninfected macrophages and RT-PCR was performed following the protocol described above.

298 **LmCas9:T7Pol *L. major* strain generation**

299 LmCas9:T7Pol expressing *L. major* cells were generated following protocols and plasmid
300 developed by Beneke et al. (Beneke et al., 2017) with slight modification. pTB007 cells were
301 electroporated into wild-type *L. major* cells. 30 µg of the plasmid was resuspended in an
302 electroporation buffer (21 mM HEPES, 0.7 mM NaH_2PO_4, 137 mM NaCl, and 6 mM glucose;
303 pH 7.4) and electroporated using BTX Gemini electroporator (480 V, 550 µF, 25 ohms) to 4
304 x10^7 *L. major* promastigotes. The cells were selected in the presence of 50 µg/ml Hygromycin.
305 Total genomic DNA was isolated from selected cells and subjected to PCR to verify the
306 generated strain. The PCR was conducted with P3/P4, P5/P6 and P7/P8 for amplification of
307 SpCas9, T7pol and rRNA45, respectively.

308 **Generation of N-terminal mNG-tagged-epsilon/alpha-tubulin expressing *L. major* strains**

309 The N-terminal mNG-tagged-epsilon/alpha-tubulin expressing *L. major* strains were generated
310 following the protocol reported by Beneke et al. (Beneke et al., 2017) and as schematically
311 described in Fig S3. The primers used for the strain generation were designed using the
312 LeishGEdit primer design module (http://www.leishgedit.net/Home.html) and the primer
313 sequences are provided in Table S2. For preparation of sgDNA (template for sgRNA), overlap

314 extension PCR was performed using primer P11 (for ε-tubulin) or P14 (for α-tubulin) and
315 primer G00 (containing sgRNA scaffold sequence). Donor DNA containing blasticidin resistant
316 gene flanked by 30 nucleotide upstream and downstream sequence of the Cas9-cleavage site
317 was PCR amplified using pPLOTv1 blast-mNG-blast plasmid as template and primers P9/P10
318 (for ε-tubulin) and P12/P13 (for α-tubulin). All the PCR amplifications were done using PFU
319 polymerase following the protocol mentioned by Beneke et al., 2017 (Beneke et al., 2017). The
320 donor DNAs were gel eluted using commercial kit (BioBharati). The eluted donor DNA and
321 corresponding sgDNA were simultaneously electroporated into LmCas9:T7Pol *L. major* cells
322 and selected in 20 μg/ml blasticidin containing media for ~7 days.

323 **Western blotting**

324 Whole cell lysate was prepared in 1X resuspension buffer (1X PBS+1X protease inhibitor
325 cocktail) with sonication. Protein amount was quantified using Lowry method and 40 μg of
326 whole cell lysate were loaded in 12% polyacrylamide gel and subjected to SDS-PAGE. The
327 protein was transferred to PVDF membrane and blocked with blocking solution (5% skim milk
328 solution in TBST (10 mM Tris, 150 mM NaCl, 0.025% Tween 20)). The membrane is washed
329 for 5 minutes for two times and incubated overnight with shaking at cold room with rabbit anti-
330 mNG primary antibody and rabbit anti-LdActin diluted in TBST (Table S3). The membrane
331 was washed with 1X TBST for 5 minutes 5 times and incubated with HRP tagged goat anti-
332 rabbit secondary antibody for 1.5 hours in room temperature. The membrane was washed with
333 1X TBST for 5 minutes for 5 times. Using chemiluminescent substrate (Biorad), blot was
334 developed and signal documented in ChemiDoc imaging system (Biorad).

335 **Imaging studies**

336 mNG-ε-tubulin expressing *L. major* promastigotes were spread on poly-L-lysine-coated
337 coverslips and incubated for 30 minutes. Fixation solution (4% paraformaldehyde in 1X PBS)
338 was added to it and incubated in dark for 10 mins. The coverslips were washed twice with 1X

339 PBS and mounted in antifade mounting media with DAPI (Vectashield). The images were
340 acquired in Leica SP8 confocal microscope using a 63X oil immersion lens. Images were
341 processed using LasX (Leica). Central 1-3 stacks were merged and projected for representation.
342 mNG-ε-tubulin expressing *L. major* amastigote inside macrophages were imaged by the same
343 protocol with slight modification. J774A.1 macrophages were infected with mNG-tagged-ε-
344 tubulin *L. major* cells as described above. At ~60 hours post infection, macrophages were fixed,
345 washed twice with 1X PBS and mounted in antifade mounting media with DAPI (Vectashield).
346 The images were acquired in Leica SP8 confocal microscope using a 63X oil immersion lens.
347 Images were processed using LasX (Leica). Central 1-3 stacks were merged and projected for
348 representation.

349 **Nocodazole disruption assay**

350 mNG-tagged-epsilon/alpha-tubulin expressing *L. major* promastigotes ($1x10^7$ cells) were
351 incubated with 1 μM Nocodazole or DMSO (as control) in 200 μl M199 media for 1 hour. Cells
352 were spread on a poly-L-lysine coated coverslip and fixed with 4% paraformaldehyde for 10
353 minutes. Coverslips were washed twice with 1X PBS, mounted in antifade mounting media
354 with DAPI (Vectashield) and imaged immediately in Leica SP8 confocal microscope.
355 Individual stacks were analyzed and represented. The percentage of cells with unaltered
356 localization of the respective tubulins (ε or α) were calculated for both untreated and
357 nocodazole treated cells. In the case of α-tubulin, the cytoskeleton is considered intact if the
358 peripheral tubulin signal is clearly visible. In the case of ε-tubulin strain, if two distinct puncta
359 are visible, it is considered as unaltered.

360 **Acknowledgment**

361 The authors thank Dr. Sankar Maiti and Dr. Subhra Majumder for sharing reagents and for
362 providing valuable suggestions. Dr. Subrata Adak and Dr. Amogh Sahasrabuddhe are
363 acknowledged for providing the plasmids for CRISPR-Cas9 manipulation and LdActin

antibody, respectively. Dr. Subhankar Dolai is thanked for his critical comments on the manuscript.

Funding

This work was supported by Indian Council of Medical Research (ICMR) research grant No: 6/9-7(318)/2023-ECD-II and West Bengal DSTBT grant No: 398(Sanc.)/STBT-13015/16/2024-ST SEC awarded to RD. AS was supported by CSIR NET fellowship.

Competing interests

No competing interests declared

Data and resource availability

All other data that supports the results of this study are available from the corresponding author (rupakdatta@iiserkol.ac.in) upon reasonable request.

References

Alexander, J. (1978). Unusual axonemal doublet arrangements in the flagellum of Leishmania amastigotes. *Transactions of the Royal Society of Tropical Medicine and Hygiene* **72**, 345–347.

Beneke, T., Madden, R., Makin, L., Valli, J., Sunter, J. and Gluenz, E. (2017). A CRISPR Cas9 high-throughput genome editing toolkit for kinetoplastids. *R. Soc. open sci.* **4**, 170095.

Brotherton, M.-C., Racine, G., Foucher, A. L., Drummelsmith, J., Papadopoulou, B. and Ouellette, M. (2010). Analysis of Stage-Specific Expression of Basic Proteins in *Leishmania infantum*. *J. Proteome Res.* **9**, 3842–3853.

Burns, R. G. (1995). Identification of two new members of the tubulin family. *Cell Motil. Cytoskeleton* **31**, 255–258.

Burza, S., Croft, S. L. and Boelaert, M. (2018). Leishmaniasis. *The Lancet* **392**, 951–970.

388 **Chang, P. and Stearns, T.** (2000). δ-Tubulin and ε-tubulin: two new human centrosomal
389 tubulins reveal new aspects of centrosome structure and function. *Nat Cell Biol* **2**, 30–
390 35.
391 **Chang, P., Giddings, T. H., Winey, M. and Stearns, T.** (2003). ε-Tubulin is required for
392 centriole duplication and microtubule organization. *Nat Cell Biol* **5**, 71–76.
393 **Dandugudumula, R., Fischer-Weinberger, R. and Zilberstein, D.** (2022). Morphogenesis
394 Dynamics in Leishmania Differentiation. *Pathogens* **11**, 952.
395 **Debrabander, M., Demey, J., Joniau, M. and Geuens, G.** (1977). Ultrastructural
396 immunocytochemical distribution of tubulin in cultured cells treated with microtubule
397 inhibitors. *Cell Biology International Reports* **1**, 177–183.
398 **Dupuis-Williams, P., Fleury-Aubusson, A., De Loubresse, N. G., Geoffroy, H., Vayssié,**
399 **L., Galvani, A., Espigat, A. and Rossier, J.** (2002). Functional role of ε-tubulin in
400 the assembly of the centriolar microtubule scaffold. *The Journal of Cell Biology* **158**,
401 1183–1193.
402 **Dutcher, S. K., Morrissette, N. S., Preble, A. M., Rackley, C. and Stanga, J.** (2002). ε-
403 Tubulin Is an Essential Component of the Centriole. *MBoC* **13**, 3859–3869.
404 **Field, M. C. and Carrington, M.** (2009). The trypanosome flagellar pocket. *Nat Rev*
405 *Microbiol* **7**, 775–786.
406 **Fong, D. and Lee, B.** (1988). Beta tubulin gene of the parasitic protozoan *Leishmania*
407 *mexicana*. *Molecular and Biochemical Parasitology* **31**, 97–106.
408 **Fourriere, L., Jimenez, A. J., Perez, F. and Boncompain, G.** (2020). The role of
409 microtubules in secretory protein transport. *Journal of Cell Science* **133**, jcs237016.
410 **Gluenz, E., Ginger, M. L. and McKean, P. G.** (2010). Flagellum assembly and function
411 during the Leishmania life cycle. *Current Opinion in Microbiology* **13**, 473–479.

Gull, K. (1999). The Cytoskeleton of Trypanosomatid Parasites. *Annu. Rev. Microbiol.* **53**, 629–655.

Halliday, C., Yanase, R., Catta-Preta, C. M. C., Moreira-Leite, F., Myskova, J., Pruzinova, K., Volf, P., Mottram, J. C. and Sunter, J. D. (2020). Role for the flagellum attachment zone in Leishmania anterior cell tip morphogenesis. *PLoS Pathog* **16**, e1008494.

Inclán, Y. F. and Nogales, E. (2001). Structural models for the self-assembly and microtubule interactions of γ-, δ- and ε-tubulin. *Journal of Cell Science* **114**, 413–422.

Ivens, A. C. (2005). The Genome of the Kinetoplastid Parasite, Leishmania major. *Science* **309**, 436–442.

Janke, C. and Chloë Bulinski, J. (2011). Post-translational regulation of the microtubule cytoskeleton: mechanisms and functions. *Nat Rev Mol Cell Biol* **12**, 773–786.

Jumper, J., Evans, R., Pritzel, A., Green, T., Figurnov, M., Ronneberger, O., Tunyasuvunakool, K., Bates, R., Žídek, A., Potapenko, A., et al. (2021). Highly accurate protein structure prediction with AlphaFold. *Nature* **596**, 583–589.

Libusová, L., Sulimenko, T., Sulimenko, V., Hozák, P. and Dráber, P. (2004). γ-Tubulin in Leishmania: cell cycle-dependent changes in subcellular localization and heterogeneity of its isoforms. *Experimental Cell Research* **295**, 375–386.

McKenna, E. D., Sarbanes, S. L., Cummings, S. W. and Roll-Mecak, A. (2023). The Tubulin Code, from Molecules to Health and Disease. *Annu. Rev. Cell Dev. Biol.* **39**, 331–361.

Nogales, E., Wolf, S. G. and Downing, K. H. (1998a). Structure of the alpha beta tubulin dimer by electron crystallography. *Nature* **391**, 199–203.

Nogales, E., Downing, K. H., Amos, L. A. and L❓we, J. (1998b). Tubulin and FtsZ form a distinct family of GTPases. *Nat Struct Mol Biol* **5**, 451–458.

Overath, P., Stierhof, Y.-D. and Wiese, M. (1997). Endocytosis and secretion in trypanosomatid parasites — Tumultuous traffic in a pocket. *Trends in Cell Biology* **7**, 27–33.

Pal, D. S., Mondal, D. K. and Datta, R. (2015). Identification of Metal Dithiocarbamates as a Novel Class of Antileishmanial Agents. *Antimicrobial Agents and Chemotherapy* **59**, 2144–2152.

Pal, D. S., Abbasi, M., Mondal, D. K., Varghese, B. A., Paul, R., Singh, S. and Datta, R. (2017). Interplay between a cytosolic and a cell surface carbonic anhydrase in pH homeostasis and acid tolerance of *Leishmania*. *Journal of Cell Science* **130**, 754–766.

Paysan-Lafosse, T., Blum, M., Chuguransky, S., Grego, T., Pinto, B. L., Salazar, G. A., Bileschi, M. L., Bork, P., Bridge, A., Colwell, L., et al. (2023). InterPro in 2022. *Nucleic Acids Research* **51**, D418–D427.

Pettersen, E. F., Goddard, T. D., Huang, C. C., Couch, G. S., Greenblatt, D. M., Meng, E. C. and Ferrin, T. E. (2004). UCSF Chimera—A visualization system for exploratory research and analysis. *J Comput Chem* **25**, 1605–1612.

Pollard, T. D. and Cooper, J. A. (2009). Actin, a Central Player in Cell Shape and Movement. *Science* **326**, 1208–1212.

Ross, I., Clarissa, C., Giddings, T. H. and Winey, M. (2013). ε-tubulin is essential in *Tetrahymena thermophila* for the assembly and stability of basal bodies. *Journal of Cell Science* jcs.128694.

Rudzinska, M. A., D'Alesandro, P. A. and Trager, W. (1964). The Fine Structure of *Leishmania donovani* and the Role of the Kinetoplast in the Leishmania-Leptomonad Transformation*. *The Journal of Protozoology* **11**, 166–191.

Selvapandiyan, A., Duncan, R., Debrabant, A., Bertholet, S., Sreenivas, G., Negi, N. S., Salotra, P. and Nakhasi, H. L. (2001). Expression of a Mutant Form of Leishmania

462 donovani Centrin Reduces the Growth of the Parasite. *Journal of Biological*
463 *Chemistry* **276**, 43253–43261.
464 **Sengupta, S., Tripathi, J., Tandon, R., Raje, M., Roy, R. P., Basu, S. K. and**
465 **Mukhopadhyay, A.** (1999). Hemoglobin Endocytosis in Leishmania Is Mediated
466 through a 46-kDa Protein Located in the Flagellar Pocket. *Journal of Biological*
467 *Chemistry* **274**, 2758–2765.
468 **Stierhof, Y. D., Ilg, T., Russell, D. G., Hohenberg, H. and Overath, P.** (1994).
469 Characterization of polymer release from the flagellar pocket of Leishmania mexicana
470 promastigotes. *The Journal of cell biology* **125**, 321–331.
471 **Sunter, J. and Gull, K.** (2017). Shape, form, function and *Leishmania* pathogenicity: from
472 textbook descriptions to biological understanding. *Open Biol.* **7**, 170165.
473 **Sunter, J. D., Yanase, R., Wang, Z., Catta-Preta, C. M. C., Moreira-Leite, F., Myskova,**
474 **J., Pruzinova, K., Volf, P., Mottram, J. C. and Gull, K.** (2019). *Leishmania*
475 flagellum attachment zone is critical for flagellar pocket shape, development in the
476 sand fly, and pathogenicity in the host. *Proc. Natl. Acad. Sci. U.S.A.* **116**, 6351–6360.
477 **Tran, K. D., Vieira, D. P., Sanchez, M. A., Valli, J., Gluenz, E. and Landfear, S. M.**
478 (2015). Kharon1 Null Mutants of Leishmania mexicana Are Avirulent in Mice and
479 Exhibit a Cytokinesis Defect within Macrophages. *PLoS ONE* **10**, e0134432.
480 **Turk, E., Wills, A. A., Kwon, T., Sedzinski, J., Wallingford, J. B. and Stearns, T.** (2015).
481 Zeta-Tubulin Is a Member of a Conserved Tubulin Module and Is a Component of the
482 Centriolar Basal Foot in Multiciliated Cells. *Current Biology* **25**, 2177–2183.
483 **van Breugel, M., Wilcken, R., McLaughlin, S. H., Rutherford, T. J. and Johnson, C. M.**
484 (2014). Structure of the SAS-6 cartwheel hub from Leishmania major. *eLife* **3**,
485 e01812.

Varadi, M., Anyango, S., Deshpande, M., Nair, S., Natassia, C., Yordanova, G., Yuan, D., Stroe, O., Wood, G., Laydon, A., et al. (2022). AlphaFold Protein Structure Database: massively expanding the structural coverage of protein-sequence space with high-accuracy models. *Nucleic Acids Research* **50**, D439–D444.

Vats, K., Tandon, R., Roshanara, Beg, Mirza. A., Corrales, R. M., Yagoubat, A., Reyaz, E., Wani, Tasaduq. H., Baig, Mirza. S., Chaudhury, A., et al. (2023). Interaction of novel proteins, centrin4 and protein of centriole in Leishmania parasite and their effects on the parasite growth. *Biochimica et Biophysica Acta (BBA) - Molecular Cell Research* **1870**, 119416.

Vaughan, S., Attwood, T., Navarro, M., Scott, V., McKean, P. and Gull, K. (2000). New tubulins in protozoal parasites. *Current Biology* **10**, R258–R259.

Wheeler, R. J., Gluenz, E. and Gull, K. (2015). Basal body multipotency and axonemal remodelling are two pathways to a 9+0 flagellum. *Nat Commun* **6**, 8964.

Wirth, D. F. and Slater, C. (1983). Isolation and characterization of an α-tubulin gene from *Leishmania enriettii*. *Molecular and Biochemical Parasitology* **9**, 83–92.

Wu, J. and Akhmanova, A. (2017). Microtubule-Organizing Centers. *Annu Rev Cell Dev Biol* **33**, 51–75.

504 **Figure Legends**

505 **Fig 1. Sequence homology of Lmε-tubulin with its counterparts in other organisms.**
506 Sequence alignment of Lmε-tubulin with epsilon-tubulins from *Homo sapiens* (Hs-ε-tubulin)
507 *Chlamydomonas reinhardtii* (Cr-ε-tubulin) *Paramecium tetraurelia* (Pt-ε-tubulin)
508 *Tetrahymena thermophila* (Tt-ε-tubulin). Yellow-shaded region indicates the GTPase domain
509 and green-shaded region indicates the C-terminal domain as predicted by InterPro analysis.
510 Residues marked by black boxes indicate lethal or slow-growing mutations in *Tetrahymena*
511 *thermophila.* Black triangles indicate GTP-binding residues of tubulins as predicted by InterPro
512 analysis.

513 **Fig 2. Genomic PCR and RT-PCR analysis of Lmε-tubulin** [A] Schematic diagram of the
514 chromosome 21 locus containing *Lmε-tubulin* and the adjacent genes. Binding sites of the Lmε-
515 tubulin-specific primers (P1/P2) are shown. [B] Agarose gel image showing PCR amplification
516 of 1413 bp *Lmε-tubulin* genomic locus with primer sets P1/P2. [C] Expression of Lmε-tubulin
517 mRNA in *L. major* promastigotes by RT-PCR using P1/P2. The lanes marked as '+RT' and
518 '−RT' represent the reactions with and without RT enzyme, respectively. [D] Workflow for
519 checking of expression of Lmε-tubulin mRNA in *L. major* amastigotes. [E] Expression of Lmε-
520 tubulin mRNA in *L. major* amastigotes by RT-PCR using P1/P2. The lanes marked as '+RT'
521 and '−RT' represent the reactions with and without RT enzyme, respectively. +IMΦ and -IMΦ
522 indicates RNA extracted from infected and uninfected macrophages, respectively.

523 **Fig 3. Localization of mNG-tagged epsilon-tubulin in promastigote and amastigote stage**
524 ***of L. major*.** [A] Cartoon diagram showing wild-type (WT) Lmε-tubulin genomic locus and
525 engineered mNG- Lmε-tubulin genomic locus following CRISPR-Cas9-mediated endogenous
526 tagging. [B] Whole cell lysates from WT, LmCas9:T7Pol and mNG-Lmε-tubulin expressing
527 *L. major* strain was subjected to SDS-PAGE and the protein expression was checked by western
528 blotting using antibody against mNG (upper), and actin (lower) as housekeeping control. An

529 81.7 kDa band corresponding to the molecular weight of the fusion protein (30 kDa: 3XMyc-
530 mNeonGreen, and 51.7 kDa: Lmε-tubulin) was detected. [C] Confocal microscopy of mNG-
531 Lmε-tubulin expressing *L. major* promastigotes. Cells were fixed and mounted in DAPI (blue)
532 containing mounting media to stain the nuclei and the kinetoplast. Green signal represents
533 mNG-ε-tubulin localization. Merged panel represent the combined image of DAPI along with
534 mNG-ε-tubulin. Merged DIC represent the fluorescent signal overlay on DIC image captured
535 simultaneously showing two distinct green signals, one in close association with the kinetoplast
536 DNA and the other at the base of the flagella. The white box represents the area that has been
537 zoomed and represented as magnified panel. The scale bar represents 10μm. The white arrow
538 represents the bright spot of mNG-ε-tubulin near kinetoplast (K) and yellow arrow represent
539 bright spot away from kinetoplast. The nucleus is marked as 'N' [D] J774A.1 macrophages
540 were infected with mNG-Lmε-tubulin expressing *L. major* cells. ~ 60 hours post infection cells
541 were fixed, and mounted with DAPI-containing mounting media and imaged in a confocal
542 microscope. Parasite nuclei (N) and kinetoplast (K) and macrophage nucleus (MϕN) were
543 stained with DAPI (blue), mNG-ε-tubulin is represented by the green signal. Merged image
544 represent the combined image of DAPI along with mNG-ε-tubulin. Merged DIC represent the
545 fluorescent signal overlay on DIC image captured simultaneously. The white box represents
546 the area that has been zoomed and represented as magnified panel. The scale bar represents
547 10 μm. Two bright spots of mNG-ε-tubulin can be seen in the amastigotes too, one closely
548 associated with the kinetoplast (white arrow) and the other distal from the kinetoplast (yellow
549 arrow).

550 **Fig 4. Nocodazole sensitivity assay for tubulins.** [A] mNG-ε-tubulin distribution in the
551 untreated (left panel) and 1 μM nocodazole treated (right panel) *L. major* promastigotes
552 expressing mNG-ε-tubulin. Nucleus and kinetoplast are stained with DAPI (blue). Green signal
553 represents mNG-ε-tubulin localization. [B] Bar graph showing percentage of cells where ε-

554 tubulin distribution remained unaltered after mock (only DMSO) or 1 μM nocodazole
555 treatment. [C] mNG-α-tubulin distribution in the untreated (left panel) and 1 μM nocodazole
556 treated (right panel) *L. major* promastigotes expressing mNG-α-tubulin. Nucleus and
557 kinetoplast are stained with DAPI (blue). Green signal represents mNG-α-tubulin
558 localization [D] Bar graph showing percentage of cells where alpha-tubulin distribution
559 remained unaltered after mock (only DMSO) or 1 μM Nocodazole treatment. At least 120 cells
560 were quantified from three independent experiments and presented as ±SD. n.s., non-
561 significant; **$p \leq 0.01$.

Figure 1

```
Lmε-tubulin     MPREIVTVQVGQCGNQLGQRWFDVMLQEHKAYPHFPE---ARDAVFL----------- 44
Hsε-Tubulin     -MTQSVVVQVGQCGNQIGCCFWDLALREHAAVNQKGIYDEAISSFFRNVDTRVVGDGGS- 58
Crε-tubulin     MPRELVTIQVGQCGNQVGCRFWELALREHAAYNTKGVYDEALSSFFRNVDTRVEPPRNLP 60
Ptε-tubulin     MPRELIFVQVGQCGNQIGMRFWDLALKEHAKAKQSLLYDESLSSFFRNVN--SKN-QELK 57
Ttε-tubulin     -MRELITIQVGQCGNQIGAKFWELAIKEHSKYNKSSVYDDALSSFFRNIDKSSKG-HELK 58
                   : : :********:*  :::: ::**           : .:.*

Lmε-tubulin     --EAMNHPGRLKARCVAVDMEQGVLHAMLRGPLKDIFDANFFVSDVSGAGNNWAVGHMEY 102
Hsε-Tubulin     --ISKGKICSLKARAVLIDMEEGVVNEILQGPLRDVFDTKQLITDISGSGNNWAVGHKVF 116
Crε-tubulin     VGEGRGAIRTLKARSVIVDMECGVINEMLKGPLGEVLDTRQLVSDVSGAGNNWAHGHHEY 120
Ptε-tubulin     IG---DPIQNLKARALIVDMEEGVINQIMKSPLGELFEERQCINDVSGAGNNWAHGFYHY 114
Ttε-tubulin     VG---SEIINLKARSIIVDMEEGVTNQLLKSDIGDLFDQRQFINDVSGAGNNWAHGHFFY 115
                     .    ****.: :*** ** : :::. : :::: .  :.*:**:***** *.  :

Lmε-tubulin     GDRYIDAIAESVRNQVEQCNCIQSFFLMHSLSGGTGSGLGTRVLGMLEDEFPHVFRICPV 162
Hsε-Tubulin     GSLYQDQILEKFRKSAEHCDCLQCFFIIHSMGGGTGSGLGTFLLKVLEDEFPEVYRFVTS 176
Crε-tubulin     GPRYHDAILDKIRLTAEDCDSLQSFMVLHSLGGGTGSGVGTYIVRMLADEFPGVFRFTGS 180
Ptε-tubulin     GNQYEKHIEERLRKTVEQCDSLQCFFMTHSIGGGTGSGLGSRIVGLLEDNYPEVFRFTAS 174
Ttε-tubulin     GNKYRDNMSERIRKAVEQCDSLQCFFLMHSLGGGTGSGLGTFLLSLIEDEYPDVYRFTAS 175
                *  * . : : .*  .*.*:.:*.*:: **:.******:*: :: :: *::* *:*:

Lmε-tubulin     VMPSEVDDVVTAPYNSCFSLKELIEHADCVLPLDNDALARMADRALSSRPQGRGVMAS-- 220
Hsε-Tubulin     IYPSGEDDVITSPYNSILAMKELNEHADCVLPIDNQSLFDIISKIDLMVNSGKLGTTV-- 234
Crε-tubulin     VFPSEDDDVVTSPYNAMLALGQLVEHADCVLPIENQALIDIVNRTEAARDRAAAADAA-- 238
Ptε-tubulin     VFPSGDDDVVTSPYNSLFSLYELAKHADCVFPIDNQALINIVDQIDKPNKARLVKENAHE 234
Ttε-tubulin     VFPQKDDDVITSPYNSFFSLYELAKHADCVFPIDNQALMNICYQIDNPNKVKLAKDNINV 235
                : *.  ***:*:***: ::: :* :*****:*::*::*  :  :

Lmε-tubulin     -S-------VPQPQAFSAAKPTDTKGLPYDSMNGLVAQLLSNLTCAMRFPGPLNMDINEI 272
Hsε-Tubulin     ----KPKSL----VTSSSGALKKQHKKPFDAMNNIVANLLLNLTSSARFEGSLNMDLNEI 286
Crε-tubulin     ------------ASAVSGLKGSGGGSKPFDSMNGVAASLLLHLTASVRFEGPLNVDLNDI 286
Ptε-tubulin     G---------SVGIKITQFGEEEKRQKPFDKMNSLIAHLLSHITCSMRFEGALNVDLNEI 285
Ttε-tubulin     SKEEEIKIMMNKGSKITQAGTEEKKEKPFDKMNNIIAHLLSNITCSMRFEGVLNVDLNEI 295
                              :           *:* **.: * ** ::*.: ** * **:*:*:*

Lmε-tubulin     TTNLVPFPRLHFLTAAIAPLSVSSK---------HAAVGPRTVDAMITACLDPGHQFVDV 323
Hsε-Tubulin     SMNLVPFPQLHYLVSSLTPLYTLT----------DVNIPPRRLDQMFSDAFSKDHQLLRA 336
Crε-tubulin     TMNLVPYPRMHFLLSSMSPLQPPPKDKDVGRAAAALALQPRTLDQVFGDVFSREHQLIRA 346
Ptε-tubulin     TMNLVPYPDLHFLISSMAPLYSLL----------DSKLQPRRLDQMFNDIYHPDFQMITG 335
Ttε-tubulin     TMNLVPYPDLHFLISSIAPLYSLS----------DSNLQPRRLDQMFKDCYHPDYQLVSV 345
                : ****:* :*:* ::::**                 : ** :* ::       .*::

Lmε-tubulin     RHGQGSAVTREAGKTLATALIARGPQTTVGDLTRGVGRLREQMEMPYWNEDGFKTALCGV 383
Hsε-Tubulin     DP--------KHSLYLACALMVRGNV-QISDLRRNIERLKPSLQFVSWNQEGWKTSLCSV 387
Crε-tubulin     DP--------RAATYLACGLIARGPTATMADINRNVARLRPQLKMVHWNSEGFKLGICST 398
Ptε-tubulin     QP--------SLHKYLAVGLLVRGDV-AFSDVNRNIKKLKDQLKMIYWNQEGFKYGICNQ 386
Ttε-tubulin     NP--------FQNKYLAVGLMVRGSV-PFSDVNRNIKKLRSELNMIYWNQEGFKYGICNT 396
                             ** .*:.**    ..*: *.: :*: .:::  **.:*:* .:*.

Lmε-tubulin     SPLGHKDSMLLLANNCSIRGKVESMLSKYERLYSVRSHVHHYDQY--LSDAYFVHTVETL 441
Hsε-Tubulin     PPVGHSHSLLALANNTCVKPTFMELKERFMRLYKKKAHLHHYLQVEGMEESCFTEAVSSL 447
Crε-tubulin     PPVGCPFGLLCLANNTAIAHTFTTMRERFDKLYKRRFYTHHYEQY--MDPGGFTSAMEVV 456
Ptε-tubulin     PPIGQQYSMLCLANNTCIKDTFQEMTDRFQKLYKRKVYVHHYKQY--MEQSHFDETLNGI 444
Ttε-tubulin     PPIGQPYSLLCLANNTAIRDQFSTMVERFNKLYKRKVFVHHYTEY--MDAKHFDEALNSI 454
                 *:*   .:* **** .:    .  : .:: :**. : . *** :   :.   *  ::. :

Lmε-tubulin     RTLVDDYAYLDTAAPPKDLPRSMKDLIYY--          470
Hsε-Tubulin     SALIQEYDQLDATKNMPVQ-DLPRLSIAM--          475
Crε-tubulin     GDLTAQYRALEGATQAPPLTRLRPRGLSFLP          487
Ptε-tubulin     QNLMVKYQDLEMAQ-PKKYQRIQPIF-----          469
Ttε-tubulin     TSLISKYEELHKAEEPSSQPRLKPLI-----          480
                  *  .*  *. :
```

Figure 2

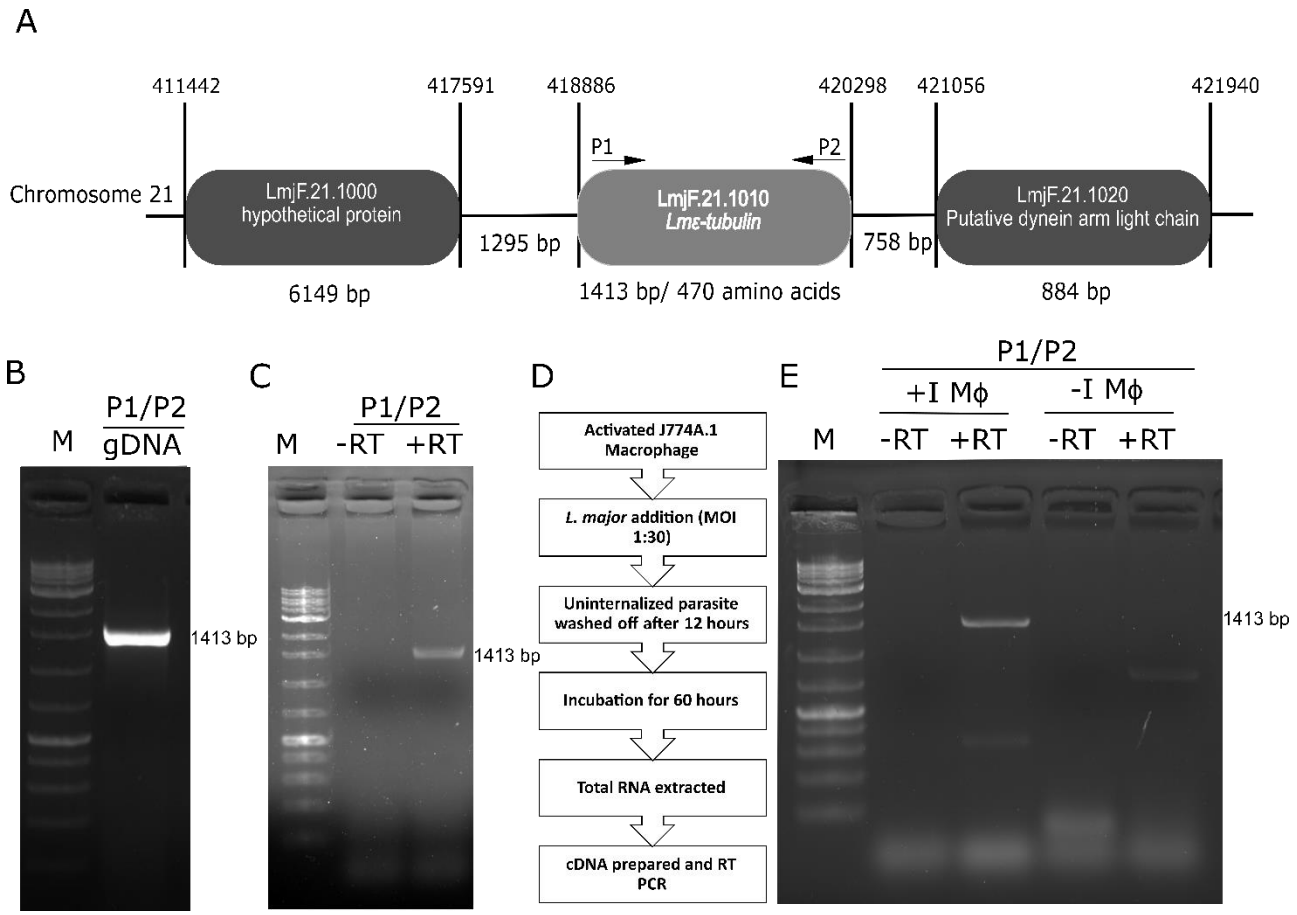
A
411442
417591
418886
420298
421056
421940
Chromosome 21
LmjF.21.1000
hypothetical protein
P1
P2
LmjF.21.1010
Lmε-tubulin
LmjF.21.1020
Putative dynein arm light chain
1295 bp
758 bp
6149 bp
1413 bp/ 470 amino acids
884 bp
B
M
P1/P2
gDNA
1413 bp
C
M
P1/P2
-RT
+RT
1413 bp
D
Activated J774A.1 Macrophage
L. major addition (MOI 1:30)
Uninternalized parasite washed off after 12 hours
Incubation for 60 hours
Total RNA extracted
cDNA prepared and RT PCR
E
P1/P2
+I Mϕ
-I Mϕ
M
-RT
+RT
-RT
+RT
1413 bp

Figure 3

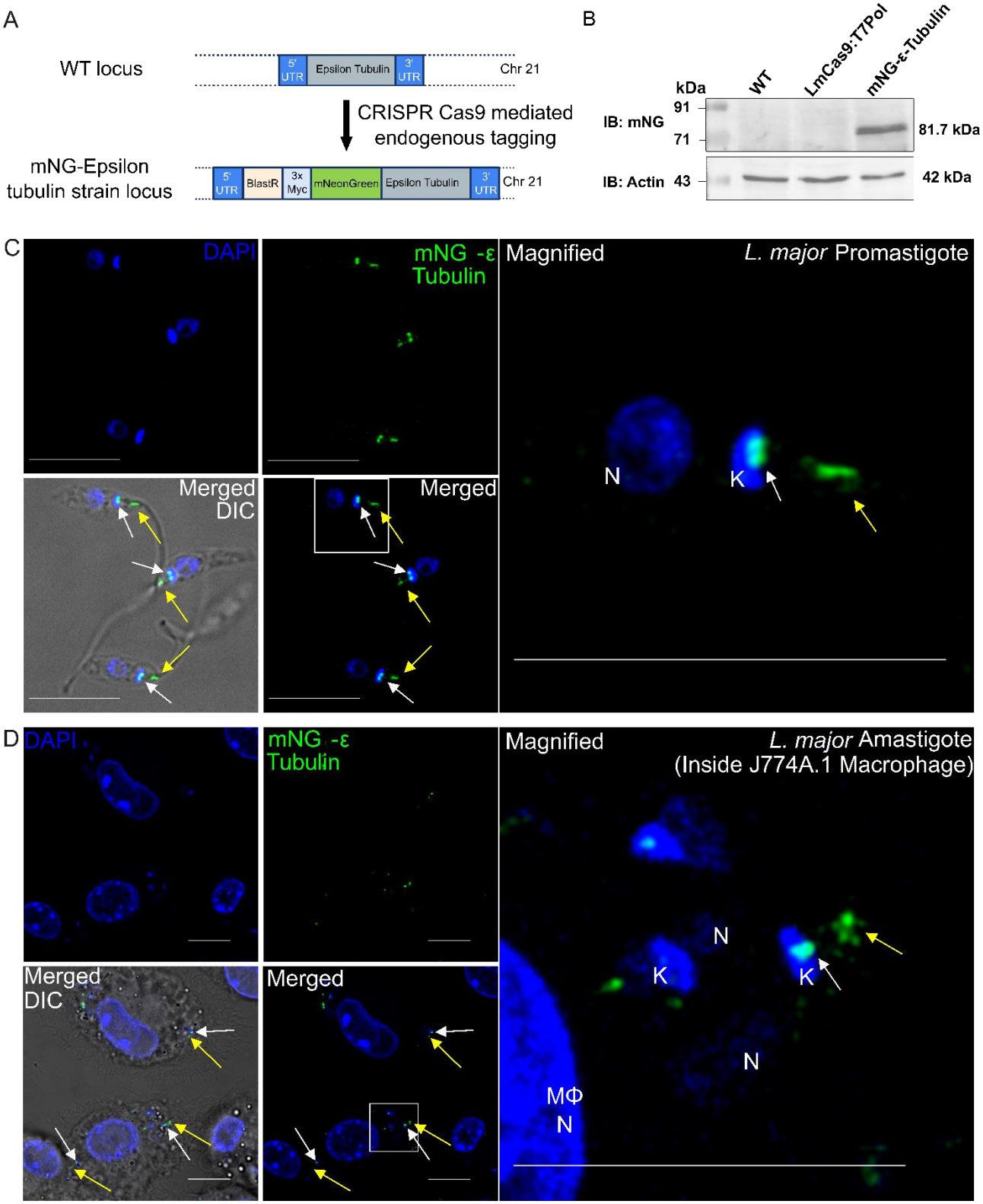
A
WT locus
5' UTR
Epsilon Tubulin
3' UTR
Chr 21
CRISPR Cas9 mediated endogenous tagging
mNG-Epsilon tubulin strain locus
5' UTR
BlastR
3x Myc
mNeonGreen
Epsilon Tubulin
3' UTR
Chr 21
B
kDa
WT
LmCas9:T7Pol
mNG-ε-Tubulin
IB: mNG
91
71
81.7 kDa
IB: Actin
43
42 kDa
C
DAPI
mNG -ε Tubulin
Magnified
L. major Promastigote
N
K
Merged DIC
Merged
D
DAPI
mNG -ε Tubulin
Magnified
L. major Amastigote (Inside J774A.1 Macrophage)
N
K
K
N
MΦ N
Merged DIC
Merged

Figure 4

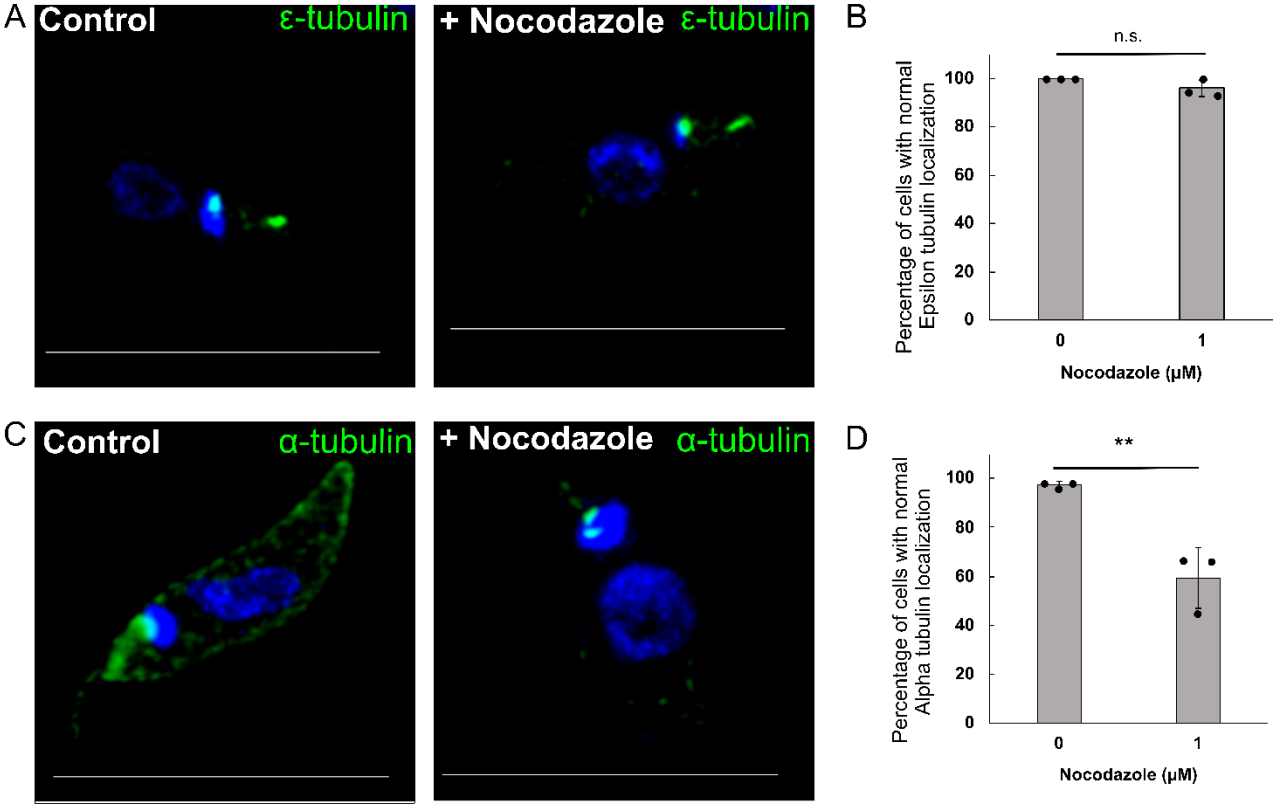
A
Control
ε-tubulin
+ Nocodazole
ε-tubulin
B
n.s.
Percentage of cells with normal Epsilon tubulin localization
100
80
60
40
20
0
0
1
Nocodazole (μM)
C
Control
α-tubulin
+ Nocodazole
α-tubulin
D
**
Percentage of cells with normal Alpha tubulin localization
100
80
60
40
20
0
0
1
Nocodazole (μM)

Supplementary information

A

```
Lmε-tubulin ---VDDVVTAPYNSCFSLKELIEHADCVLPLDNDALARMADRALSSRPQGRGVMASSVPQ     224
Lmγ-tubulin RGGESDVIVQPYNSLLAVKRLTLHADCVVVLDNTALNRIVTDNLHI--------------     222
Lmα-tubulin ---VSTAVVEPYNCVLSTHSLLEHTDVATMLDNEAIYDLTRRSLDI--------------     219
Lmβ-tubulin ---VSDTVVEPYNTTLSVHQLVENSDESMCIDNEALYDICFRTLKL--------------     217
                 . .:. ***  :: : *  ::*    :** *:  :    *

Lmε-tubulin PQAFSAAKPTDTKGLPYDSMNGLVAQLLSNLTCAMRFPGPLNMDINEITTNLVPFPRLHF     284
Lmγ-tubulin ------------ASPTVEQMNGLVSTVMAASTATLRYPGYMNNDLMSMLASLIPTPRCHF     270
Lmα-tubulin ------------ERPSYTNVNRLIGQVVSSLTASLRFDGALNVDLTEFQTNLVPYPRIHF     267
Lmβ-tubulin ------------TTPTFGDLNHLVAAVMSGVTCCLRFPGQLNSDLRKLAVNLVPFPRLHF     265
                                .:* *:. :::  *. :*: * :* *: .: ..*:* ** **

Lmε-tubulin LTAAIAPLSVSSKHAAV--GPRTVDAMITACLDPGHQFVDVRHGQGSAVTREAGKTLATA     342
Lmγ-tubulin VCTGYTPTTLDTSNIQSSVRKTSVHDVMRRLLMPKNMMVSTS--------MKSGCYISLL     322
Lmα-tubulin VLTSYAPVVSAEKA---YHEQLSVADITNSVFEPAGMLTKCD--------PRHGKYMSCC     316
Lmβ-tubulin FMMGFAPLTSRGSQ---QYRGLSVAELTQQMFDAKNMMQAAD--------PRHGRYLTAS     314
            .  . :*     .         :*  :    :     :             . *  ::
```

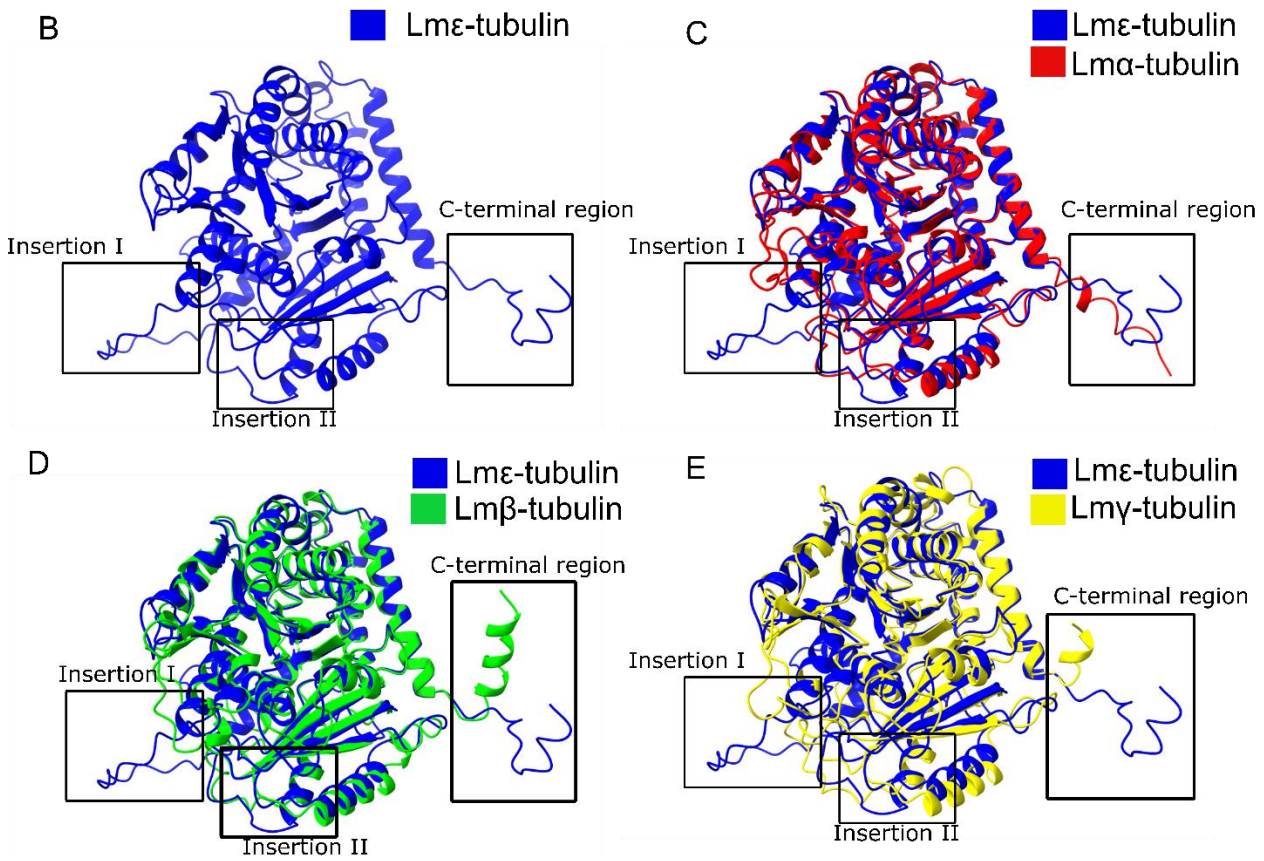

Fig. S1. Sequence and structural alignment of Lmε–tubulin with other conventional tubulins of *L. major*. [A] Lmε-tubulin (168-342) protein sequence was aligned with Lmα-tubulin (177-316), Lmβ-tubulin (175-314) and Lmγ-tubulin (177-322). Although the complete sequence of all the tubulins were aligned, only a portion of the sequence (the exact region mentioned in parenthesis) are represented in the figure. The regions shaded red indicate insertions in Lmε-tubulin that are absent in α, β or γ-tubulins, Insertion I- R211-T236, Insertion II- H325-T332. [B] AlphaFold-predicted structure of Lmε-tubulin, Insertion I, Insertion II and the C-terminal region are marked with boxes. Structural alignments of AlphaFold structure of Lmε-tubulin with that of AlphaFold structures of [C] Lmα-tubulin, [D] Lmβ-tubulin, [E] Lmγ-tubulin. All the structures aligned well with Lmε-tubulin except for three regions, Insertion I, Insertion II and the C-terminal tail.

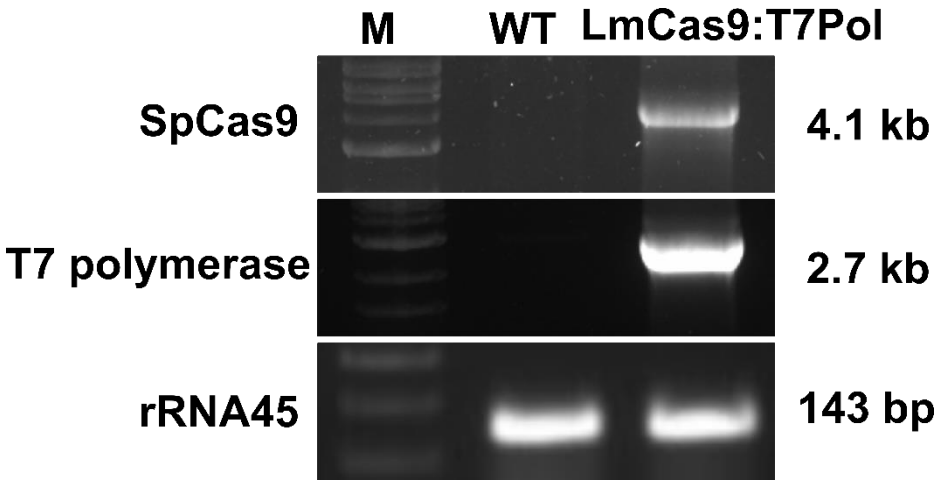

Fig. S2. Verification of LmCas9:T7Pol *L. major* strain. Presence of SpCas9 and T7 polymerase gene in the genome of LmCas9:T7Pol *L. major* cells was checked by PCR. PCR was performed with genomic DNA from wild-type (as negative control) or LmCas9:T7Pol *L. major* cells as templates with specific primers for SpCas9 and T7 Polymerase. 4.1 kb (for SpCas9) and 2.7 kb (for T7 Pol) PCR products in the LmCas9:T7Pol *L. major* cells but not in the WT confirmed proper generation of the strain. PCR for the housekeeping gene rRNA45 was used as loading control.

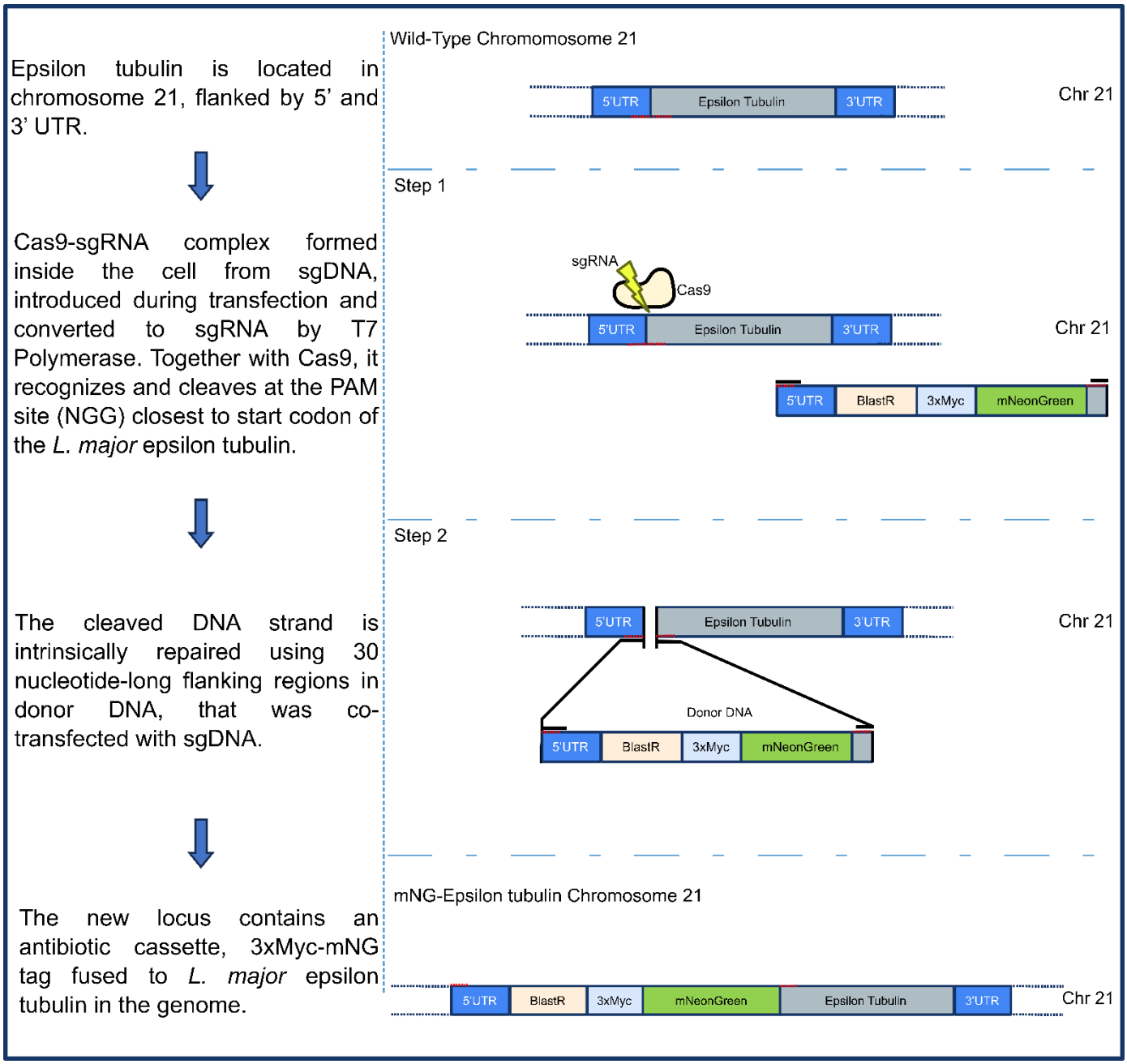

Fig. S3. Scheme for generation of mNG- Lmε-tubulin expressing *L. major* strain. Steps for generation of the N-terminal mNG-tagged-Lmε-tubulin expressing *L. major* strain employing CRISPR-Cas9 endogenous tagging method are described schematically.

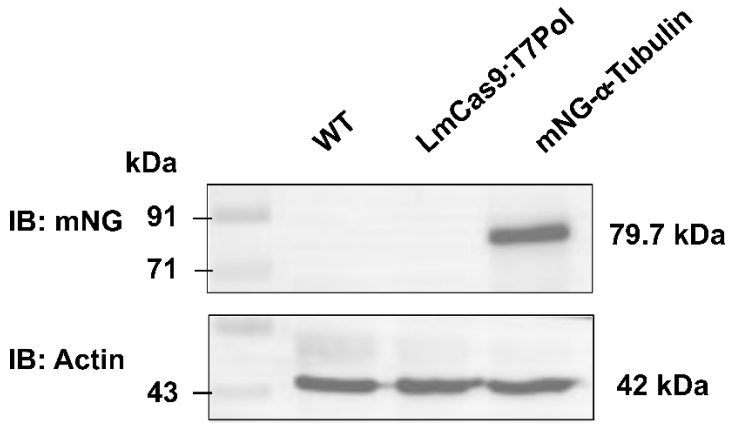

Fig S4. Confirmation of the mNG-Lmα-tubulin expressing *L. major* strain by western blot. Whole cell lysate from wild-type (WT), LmCas9:T7Pol and mNG- Lmα-tubulin expressing *L. major* strain was subjected to SDS-PAGE and the protein expression was checked by western blotting using antibody against mNG (upper), and actin (lower) as housekeeping control. A 79.7 kDa band corresponding to the molecular weight of the fusion protein (30 kDa: 3XMyc-mNeonGreen, and 49.7 kDa: Lmα-tubulin) was detected.

Table S1. Percentage identity and similarity of Lmε-tubulin with other organisms

Genus	Species	Percentage identity with *L. major* (%)*	Percentage similarity with *L. major* (%)*
Tetrahymena	*T. thermophila*	40.97	59.43
Chlamydomonas	*C. reinhardtii*	43.83	60.08
Homo	*H. sapiens*	41.37	59.04
Paramecium	*P. tetraurelia*	41.65	61.31
Leishmania	*L. donovani*	98.72	99.15
	L. infantum	98.72	99.15
	L. mexicana	97.23	98.51
	L. braziliensis	91.06	95.96
Trypanosoma	*T. brucei*	68.24	80.12
	T. cruzi	66.80	82.35

***Percentage identity and similarity calculated using NCBI blast**

Table S2. Oligonucleotides used in this paper

Oligo	Primer Sequence (5'-3')	Purpose
G00	AAAAGCACCGACTCGGTGCCACTTTTTCAAGTTGATAACGGACTAGCCTTATTTTAACTTGCTATTTCTAGCTCTAAAAC	Reverse primer for preparation of sgDNA
P1	ATGCCCCCGCGAAATCGTG	Epsilon tubulin forward primer
P2	TTAGTAGTAGATGAGATCCTTCATGCTGCG	Epsilon tubulin reverse primer
P3	GACAAGAAGTACAGCATCGGCCTG	Full-length primer for verification of SpCas9 presence in the genome
P4	GTCGCCTCCCAGCTGAGA	
P5	ATGGAGACGATTAACATCGCTAAGAAC	Full-length primer for verification of T7 pol presence in the genome
P6	CTACGCGAACGCGAAGTC	
P7	CCTACCATGCCGTGTCCTTCTA	rRNA45 primer (used as housekeeping gene)
P8	AACGACCCCTGCAGCAATAC	
P9	TCCACCTTGCCGTGCGCGTGCGTGTGGCCAGTATAATGCAGACCTGCTGC	Upstream forward primer for epsilon tubulin
P10	GACCTGCACCGTCACGATTTCGCGGGGCATACTACCCGATCCTGATCCAG	Upstream reverse primer for epsilon tubulin
P11	GAAATTAATACGACTCACTATAGGGGTGGGACCTTGAGCAGCGCGTTTTAGAGCTAGAAATAGC	Forward primer for preparation of sgDNA against 5' of epsilon tubulin gene
P12	CTCGTTCTTCGAACAAACACCTTTAAACCGGTATAATGCAGACCTGCTGC	Upstream forward primer for alpha tubulin
P13	GCCGATGTGGATGCAGATAGCCTCACGCATACTACCCGATCCTGATCCAG	Upstream reverse primer for alpha tubulin
P14	GAAATTAATACGACTCACTATAGGAAGAAAGAGGGGTTGGAAGGGTTTTAGAGCTAGAAATAGC	Forward primer for preparation of sgDNA against 5' of alpha tubulin gene

Table S3. Antibodies used in this study

Antibody	**Host**	**Source**	**Catalogue Number**	**Dilution**
mNeonGreen Tag Antibody	Rabbit	Cell Signaling Technology	53061S	WB- 1:1000
Anti-α-Tubulin Antibody	Rabbit	Bio Bharati Life Science	BB-AB0118	IF- 1:1000
Anti-γ-Tubulin antibody	Mouse	Sigma-Aldrich	T5326	IF- 1:100
Anti-Ld Actin	Rabbit	Gifted by Dr. Amogh Sahasrabuddhe (CSIR-CDRI)	-	WB- 1:20000
Goat Anti-rabbit Alexa-568	Goat	Invitrogen	A11011	IF- 1:800
Goat Anti-mouse Alexa-568	Goat	Invitrogen	A11001	IF- 1:800
Goat Anti-Rabbit I_gG-Peroxidase	Goat	Sigma Aldrich	A9169	IF- 1:4000